



An Improved Hierarchical Control Structure for Robust Microgrid Operation and Seamless Mode Transfer under Linear and Nonlinear Loads conditions

A. Norozpour Niazi, N. Vasegh*, A. A. Motie Birjandi

Department of Electrical Engineering, Shahid Rajaee Teacher Training University, Tehran, Iran

PAPER INFO

Paper history:

Received 25 June 2021
Received in revised form 30 July 2021
Accepted 04 August 2021

Keywords:

Adaptive Lookup Table Control
Hierarchical Control
Micro-Grid
Nonlinear Loads
Proportional Controller
Multi-resonance Controller

ABSTRACT

This paper proposes the improved hierarchical-based control of microgrid based on proportional and multi-resonance controllers to compensate for harmonic distortion of nonlinear loads. Moreover, the probable transition of MG, especially from grid-connected to unplanned islanding and unintentional MG resources outage were studied. In current and voltage controllers of three-phase VSIs which are located in the inner level, the proportional and multi-resonant controllers are implemented. To attain proper decoupled (P-Q) power-sharing, a selective harmonic type virtual impedance, and a droop-based control are implemented at the primary level. Next, to reach better restoration and subsequently, seamless transition in accidental islanding, unintentional MG-DG's outage, and synchronization process, the advanced three-phase SRF-PLL with in-loop MAF along with a simple adaptive lookup table are implemented in the secondary level of the control. The MATLAB/Simulink simulation results verified that the proposed method improved the performance of control, effectiveness, and robustness in upstream or local grid variation.

doi: 10.5829/ije.2021.34.09c.14

NOMENCLATURE

ω_c	Cut-off frequency	$G_p(s), G_q(s)$	Droop PI controller transfer functions
ω_f	Fundamental frequency	$K_{pp}, K_{lp}, K_{pq}, K_{lq}$	Droop PI controller parameters
$K_{pc}, K_{r, ch}$	Proportional- resonant coefficients of the current controller	$G_c(s)$	Current controller transfer function
$K_{pv}, K_{r, vh}$	Proportional-resonant coefficients of the voltage controller	$G_v(s)$	Voltage controller transfer function
h	Harmonic component	$G_{PWM}(s)$	PWM inverter transfer function
T_s	Time sampling	$G_{cap}(s)$	Capacitor transfer function
C, L, R	Capacitor, inductor, and resistor of LC filter	$G_L(s)$	Inductance transfer function
τ_{ff}	Feed-forward time constant	$G_{ff}(s)$	Feed-forward transfer function
f	Frequency	$R_{v, f}^+$	Fundamental positive sequence of virtual resistance
P	Active power	$R_{v, h}$	Harmonic negative and positive sequence of virtual resistance
Q	Reactive power	$L_{v, f}^+$	Fundamental positive sequence of virtual inductance
$I_{\alpha, f}^+, I_{\beta, f}^+$	Fundamental positive sequences of output current	$K_{PF, syn}, K_{IF, syn}$	PI controller parameters of the frequency synchronization loop
$I_{\alpha, h}, I_{\beta, h}$	Harmonic negative and positive sequences of output current	$K_{PE, syn}, K_{IE, syn}$	PI control parameters of the voltage synchronization loop
$V_{va}, V_{v\beta}$	Virtual voltage in $\alpha\beta$ frame	$K_{PF, res}, K_{IF, res}$	PI control parameters of the frequency restoration loop
E	Voltage	$K_{PE, res}, K_{IE, res}$	PI control parameters of the voltage restoration loop

*Corresponding Author Institutional Email: n.vasegh@stru.ac.ir (N. Vasegh)

Please cite this article as: A. Norozpour Niazi, N. Vasegh, A. A. Motie Birjandi, An Improved Hierarchical Control Structure for Robust Microgrid Operation and Seamless Mode Transfer under Linear and Nonlinear Loads conditions, International Journal of Engineering, Transactions C: Aspects, Vol. 34, No. 09, (2021) 2167-2179

MG	Micro-Grid	DER	Distributed Energy Resource
IM	Island Mode	MPC	Model Predictive Control
GCM	Grid-Connected Mode	PLL	Phase Locked-Loop
MSOGI	Multiple Second-Order Generalized Integrator	SRF-PLL	Synchronous Reference Frame Phase Locked-Loop
VIL	Virtual Impedance Loop	VSI	Voltage Source Inverter
SHVI	Selective Harmonic Virtual Impedance	MAF	Moving Average Filter
POI	Point of Interconnection	PI	Proportional-Integral
LPF	Low-Pass Filter	PR	Proportional-Resonant
FLL	Frequency-Locked Loop	QSG	Quadrature Signal Generator
CCS	Central control structure	DCS	Decentral Control Strategy
HCS	Hierarchical control structure	THD	Total Harmonic Distortion

1. INTRODUCTION

In recent years, because of environmental problems, energy crises, and rising concerns about traditional fossil energy shortages, and others, renewable energy has drawn significant attention from researchers. Hence, power systems have undergone a revolution to guarantee sustainable development and resolve power resource challenges, especially in remote areas. Moreover, the other choice to integrate different varieties of energy resources and power electronics interfaced with units is Microgrid. As a dependable electrical system, it can work in both island mode and grid-connected mode to support the main grid, remote areas, and sensitive loads [1]. Hence, variations on power system configuration such as the load variation, MG's unit connection/disconnection, and alteration in MG operation mode in the POI are some of the significant challenges. These variations on power system configuration will make frequency, phase angle, and voltage amplitude mismatches. These mismatches may result in the inrush currents and voltage spikes and consequently, the probable transition will occur [2].

Furthermore, central, decentral, and hierarchical control are the relevant control structures that are proposed to the MG control. The first one is a good choice for the MGs with joint points to have cooperation for their targets. Although in a microgrid with CCS, the operational cost is reduced, but high bandwidth for communication links is needed in MG with DER to make assurance a satisfactory dynamic response of the system. Similarly, preparing high-speed communication links among subsets will cost for the MG owners. As the central control strategy is dependent on fault/delay, consequently probable MG failure may result. This feature represented that it has low reliability [3-4]. Whereas, based on local measurements of DER in decentral control strategy, the control of MG has happened, independently. Therefore, it is made plug-and-play capability for the MG's DER. Likewise, a completely decentral control strategy is not possible to control multiple DGs because of the potent coupling through their operations in MG. Then, the robustness of DCS in MG with the distributed system is small [5-6]. Therefore, the HCS is proposed to enhance efficiency, reliability, control capability, and operation cost. Also, it

can use different resources based on different capacities, topologies, and technologies organized in MG [7-9].

As the MG can operate in two modes of operation; grid-connected ($P-Q$) and islanded ($V-f$) modes, then the operational control mode is important. In grid-connected mode, the MG is responsible to generate the demanded power into the upstream network. But for the remote areas and in a network with failure or major disturbance, to cover sensitive/local loads, the operation mode is changed and switched to unintentional/intentional islanding. So, it should have the capability to control the $V-f$ of the local region to make uninterruptable support. Consequently, a smooth transition among GCM to IM of MGs is imperative.

The other reason for MG and power system transitions is load type. There are different load types in power system such as linear [10-13], nonlinear [2, 8, 9], balanced [2, 11], unbalanced [3, 14] loads. Two adaptive and smart controllers are planned to regulate the MG frequency and voltage accurately in IM [10]. Moreover, the implemented controllers which are based on modified droop controllers are depending on MPC and H-infinity manners to ensure the smooth transition between IM and GCM. Moradi et al. [11] have studied the loads' variation, their effect on deviations of frequency and voltage, and stability issues. Then, to reach seamless transition and enhance its operation, an adopted technique for operation mode is designed and implemented. Plus, the system robustness is enhanced by gains regulation of the control loops via a fuzzy-based controller. The PR type control was designed in the inner level to track the reference current with zero steady-state error [12]. In addition, to remove the frequency deviation and ensure equal power-sharing, a restoration loop and droop controller are employed. As the power network and microgrids are regularly under linear and balanced load conditions and consequently without any harmonic distortion, to make restoration and synchronization in such system. The only positive sequence of fundamental components were reported in literature [10-14]. A master-slave controller type was proposed by Imran et al. [15]. The master is composed of hybrid battery-diesel resources. As is mentioned heretofore, the communication links with high bandwidth are needed in the central controller which will cost for the owners.

Now, by increasing the presence of the nonlinear loads in the power system, ignoring their effects is inevitable, especially during unintentional islanding and unplanned variation on a grid configuration. Likewise, power quality and after that distortion on voltage and current are the other issues of networks with nonlinear load conditions, which make the implementation of seamless transition more difficult. Because it is imposed on the voltage and power-sharing loops during the operation of a microgrid. Furthermore, under nonlinear load conditions, the SRF control type can include proportional and resonant terms to make harmonic tracking and after that harmonic compensation. Moreover, the PLL is the other key part in MG control, synchronization, and restoration to estimate phase angle, frequency, and voltage amplitude. Then, choosing appropriate PLL is essential to carry out the smooth transition. Indeed, the SRF-PLL is one of the standard PLL and is normally used in three-phase applications, in a power system with a balanced voltage and without any harmonic distortion. But its efficiency and capability in filtering the voltage disturbances in a grid with harmonic distortion and unbalanced voltage are low. Consequently, many advanced SRF-PLLs with high competence to reject the disturbance are introduced which contain different in loop filters and prefilter [16-19]. Here, the synchronous reference frame phase locked-loop with in-loop MAF designed in the last study [8] is applied which has high efficiency in harmonic distortion.

Besides, making decoupled and harmonic power-sharing is the other issue that affects the seamless transition. Therefore, a VIL is needed to achieve decoupled active and reactive power-sharing. Here, SHVI is implemented to have harmonic power-sharing in MG [20-23]. In this study, to extract the fundamental positive sequence and harmonic positive and negative sequence components of the VSIs output current, the MSOGI module is applied, too. The research contributions are:

- Proposing the control scheme based on the hierarchical structure in three-phase VSIs type microgrid and compensation of the harmonic.
- Making decoupled harmonic power-sharing (P-Q) based on fundamental and harmonic components by applying droop control, SHVI, and MSOGI in the level of primary.
- Study the effect of unintentional resources outage on MG.
- Implementing a simple lookup table in adaptive control of voltage and frequency restoration loop to restore the system.
- Finally, achieve smoother transition in the variation of system configuration, especially load connections, accidental DG outage, and variation from grid-connected mode to unintentional islanding mode.

The organization of this paper is: the hierarchical

control structure of the microgrid is represented in section 2 and the details of the control levels are stated, there. In this study, based on the load features and needs to compensate harmonic distortion, PR current and voltage controllers are implemented in the inner level. Next, the primary level contains droop control and selective harmonic virtual impedance loops. In addition, the secondary level consists of adaptive-based restoration and synchronization loops on voltage and frequency, which is applied by a simple lookup table and synchronous reference frame phase-locked-loop. After that, the achieved results of the simulation are represented in section 3 which proves the utility and correctness of the hierarchical-based structure of the proposed scheme. It is concluded at the end of this study.

2. MICROGRID HIERARCHICAL CONTROL STRUCTURE

As referred to literature [1, 8, 9], according to ANSI/ISA-95 standard, the structure of MGs hierarchical control can be arranged into four levels: the inner level with two control loops which consists of voltage and current controllers, the primary level that can contain virtual impedance and droop control, the secondary level which comprises restoration and synchronization loops, and finally territory level that includes economically optimal operation, power management, and power market. Here, the concentration of the hierarchical-based structure of the proposed scheme is on the inner, primary, and secondary levels.

2.1. Inner Control Level As is mentioned before, this level contains two loops and controllers: the interior and exterior loops which comprehend the current and voltage controllers inside of them, respectively. Here, it should be mentioned that to get a faster and better response, the speed of the interior loop is higher than the exterior one. Generally, the two-dimensional frames which are used are the stationary frame ($\alpha\beta$) and synchronous reference frame (dq). As one of the traits of the frame of dq is that it eventuates easier filtering and controlling procedure by making the DC control variables, the dq-SRF is used to transform current and voltage waveforms toward a reference frame synchronously with the power network voltage. Therefore, PI controller is the proper candidate for the dq structure. But this type of controller has a problem in tracking non-dc variables and subsequently failing to remove the steady-state error. So, the PR type control based on the stationary frame is generally preferred especially in the case of the grid with nonlinear load, issues of the power quality in the form of harmonic distortion, and consequently the necessity to make harmonic compensation [3]. As it is presented in Figure

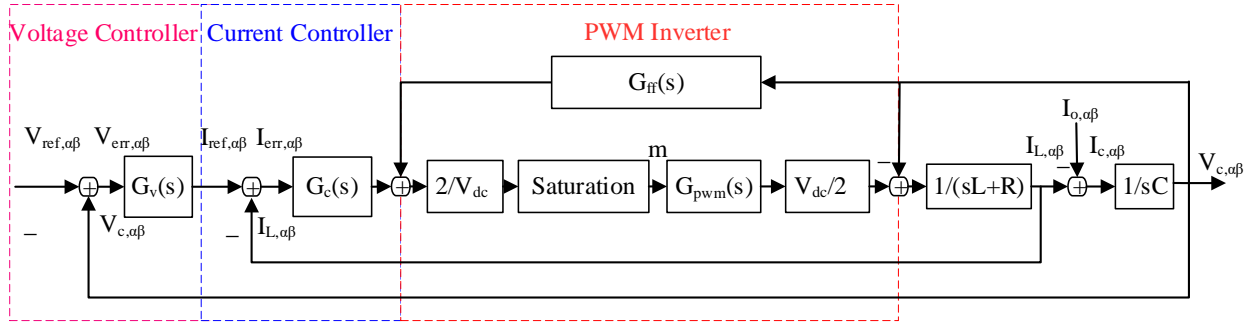


Figure 1. The control scheme of the inner control level of the VSI

1, the inner control level of the VSI has two sections; the LC filters and a microgrid control system with two loops and controllers.

2. 1. 1. Proposed Proportional and Multi-Resonance based Controller in Microgrid and Harmonic Compensation

As is mentioned before, the dq and $\alpha\beta$ frames are the key-frames that are extensively used in the power system which prepare easier controls and analysis. Since the proportional and integral controller has limitations in tracking non-DC variables and sinusoidal waveforms which resulted in a restriction to remove the steady-state error, the PR controllers are superseded controllers in the case of MG and distributed system in many studies; especially in a power system with nonlinear load condition and subsequently power quality issues [1, 12, 20-25]. As it is represented before, the control scheme of the inner control level of the VSI is presented in Figure 1. Here, in an islanded MG under nonlinear loads situations, the power quality issues should be considered. To implement them, in both current and voltage control loops, the PR-based controllers are proposed to track harmonic components of distorted voltages and currents as follow:

$$G_c(s) = K_{P,c} + \sum_{h=1,5,7,11,\dots} \frac{K_{r,ch}s}{s^2 + 2\omega_c s + (h\omega_f)^2} \quad (1)$$

$$G_v(s) = K_{P,v} + \sum_{h=1,5,7,11,\dots} \frac{K_{r,chs}}{s^2 + 2\omega_c s + (h\omega_f)^2} \quad (2)$$

$$G_{PWM}(s) = \frac{1}{1+1.5Ts} \quad (3)$$

$$G_{cap}(s) = \frac{1}{Cs} \quad (4)$$

$$G_L(s) = \frac{1}{R+Ls} \quad (5)$$

$$G_{ff}(s) = \frac{1}{1 + \tau_{ff}s} \quad (6)$$

As it is represented by Norozpour Niazi et al. [8], the bode diagrams of the control scheme of Figure 1 should be assessed to regulate the parameters of the PR controllers. As it is presented there, to define these controller parameters which are located in internal and external loops and reach a reasonable proficiency, closed-loop stability of the system, and make small steady-state errors, the internal loop should be faster than the external one by defining smaller control system closed-loop bandwidth (near ten times smaller than switching frequency of the VSC). Similarly, the external loop should be slower than the internal loop, to prevent unstable control occur. In addition, the preferred tolerable range of phase margin is 30° to 60° [26].

2. 2. Primary Control Level The primary control level has two parts: the droop-based control and virtual impedance loop; to make accurate reference voltage by online creation of the frequency and amplitude of the voltage. Additionally, to achieve power with high reliability, the responses of primary control level to grid variation should be adequately fast.

2. 2. 1. Droop Control As is presented in Figure 2 and Equations (7)-(12) based on droop control, the sharing powers are attained by measuring the output current and voltage of the VSI [27]. Hence, according to instantaneous active and reactive powers, the amplitude and frequency of the reference signal are made. These calculated instantaneous powers have AC and DC components that necessitate the use of the LPF to make the fundamental-based powers extraction which is presented in Figure 2.

$$P = V_{c\alpha}I_{o\alpha} + V_{c\beta}I_{o\beta} \quad (7)$$

$$Q = V_{c\beta}I_{o\alpha} - V_{c\alpha}I_{o\beta} \quad (8)$$

$$f = f^* - G_p(s)(P - P^*) \tag{9}$$

$$E = E^* - G_q(s)(Q - Q^*) \tag{10}$$

$$G_p(s) = \frac{K_{Pp}s + K_{Ip}}{s} \tag{11}$$

$$G_q(s) = \frac{K_{Pq}s + K_{Iq}}{s} \tag{12}$$

where * represents the reference component

2. 2. 2. Selective Virtual Impedance Loop As is mentioned in the former research [8], to make better-decoupled power-sharing (P-Q), the SHVI loop has been proposed in this study, too. It should be mentioned that virtual resistance will cause an increase in the damping of a system without any losses on proficiency while

virtual inductance will reduce power oscillation and current circulation among VSIs, increase the stability of the systems, and improve the act of decoupling in active and reactive power-sharing. Moreover, the harmonic voltage drops of lines and filter impedances can be compensated by virtual admittance [28]. Therefore, the primary current peak at the PCC is detracted and restricted by the output impedance which is increased through a virtual impedance. Hence, it makes simple DG plug-and-play capability and system stability [20]. Figures 3-4 and Equations (13)-(14) are represented that how the SHVI is added to the droop reference signal through MSOGI-FLL.

$$V_{v\alpha} = R_{v,f}^+ I_{o\alpha,f}^+ - \omega_f L_{v,f}^+ I_{o\beta,f}^+ + \sum_{h=1,-5,7,-11,13,\dots} (R_{v,h} I_{o\alpha,h}) \tag{13}$$

$$V_{v\beta} = R_{v,f}^+ I_{o\beta,f}^+ + \omega_f L_{v,f}^+ I_{o\alpha,f}^+ + \sum_{h=1,-5,7,-11,13,\dots} (R_{v,h} I_{o\beta,h}) \tag{14}$$

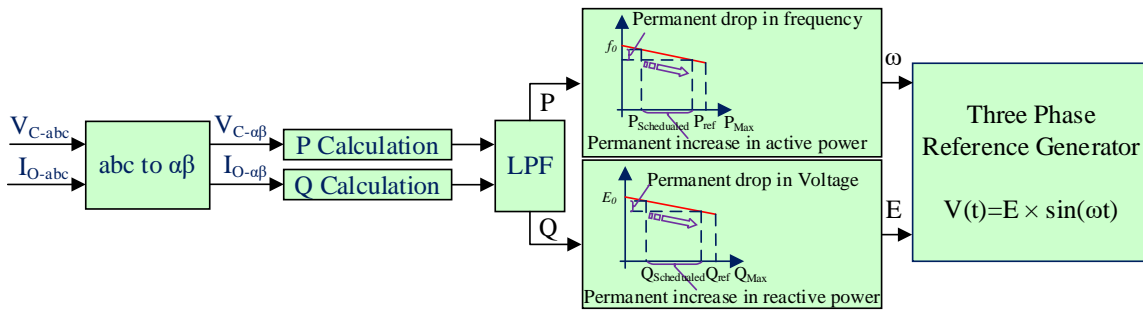


Figure 2. The block diagram of droop-based primary control scheme

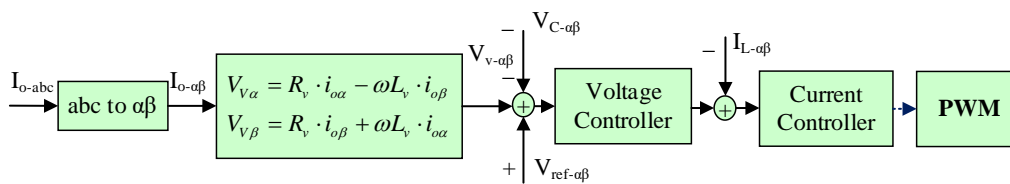


Figure 3. The block diagram of the virtual impedance loop (αβ frame).

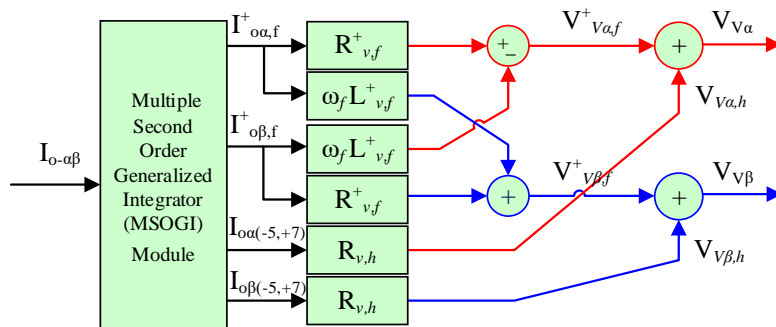


Figure 4. The block diagram of selective harmonic virtual impedance by MSOGI-FLL (αβ frame)

Moreover, it is denoted in [8, 29, 30] that to make extraction on the fundamental positive sequence and the harmonic components of the VSI output current, an

M SOGI-FLL is used. A typical block diagram M SOGI via a collection of parallel adaptive and selective filters which is tuned at the fundamental and different harmonic frequency in the frame of $\alpha\beta$ is represented in Figure 5. Here, to find the fundamental frequency of the input current, a linked FLL to the SOGI-QSG is implemented, and to set the frequencies of them, the foreseeable frequency is applied with multiplying harmonic order to the frequency. Next, this structure is used to have different harmonic components detection of the input current [30].

2. 3. Secondary Control Level

This level consists of two sections: synchronization and restoration; to attain zero steady-state error, frequency and voltage variation caused by the configuration of the grid, load changes, and droop controller.

Indeed, the restoration loop is required in the islanding mode operation of the MG to the frequency and voltage restoration. Moreover, to connect the DGs in MG and MG to the main grid, a synchronization loop is necessary [31].

2. 3. 1. Synchronization Control Loop in the Islanded MG

To synchronize the DGs of MG and/or synchronize the microgrid with the upstream power system, a loop of synchronization is needed [32]. Here, to make the accurate frequency and voltage amplitude extraction of the energy resources and accordingly smooth transitions during the synchronization, the SRF-PLL with in-loop MAF is a good candidate for a distorted voltage which is discussed in our last study [8], too. As it is mentioned there, one of the abilities of the MAF is that the dc component is passed by them. The other capability is that it can block all harmonic components whose frequencies are integer multiples of $(1/T_\omega)$. The SRF-PLL control loop with MAF has a high ability to make disturbance rejections. Figure 6 shows the block diagram of the synchronous reference frame phase locked-loop with in-loop MAF. In addition, the equations of frequency and voltage synchronization are as follows:

$$\omega_{syn} = \frac{K_{PF,syn}s + K_{IF,syn}}{s} (\omega^* - \omega_{SRF-PLL}) \tag{15}$$

$$E_{syn} = \frac{K_{PE,syn}s + K_{IE,syn}}{s} (E^* - E_{SRF-PLL}) \tag{16}$$

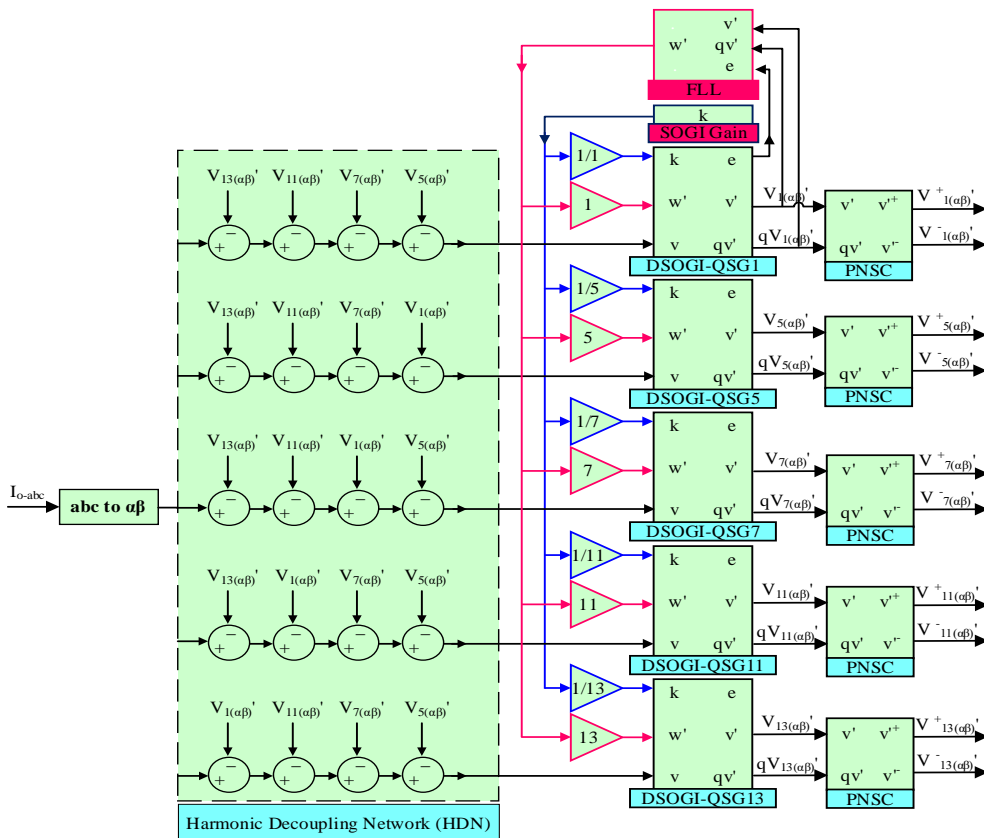


Figure 5. A typical block diagram of applied MSOGI ($\alpha\beta$ frame)

2. 3. 2. Frequency and Voltage Restoration in the Islanded MG

As is clear, one of the weaknesses of drop control is that it needs the frequency and voltage restoration to restore the voltage amplitude and frequency deviations to nominal values which are represented in Equations (17)-(18) and Figure 2.

$$\omega_{res} = \frac{K_{PF, res} s + K_{IF, res}}{s} (\omega^* - \omega_{SRF-PLL}) \tag{17}$$

$$E_{res} = \frac{K_{PE, res} s + K_{IE, res}}{s} (E^* - E_{SRF-PLL}) \tag{18}$$

It should be noted that the maximum frequency deviations based on the Nordel standard (North of Europe) and coordination of transmission of electricity union (Continental Europe) are 0.1 Hz and 0.3 Hz, respectively. Moreover, a maximum 10% deviation from the nominal value is defined for the voltage. Thus, the signal of restoration should be restricted to permissible

frequency and amplitude of voltage deviations [20]. Figure 7 shows the implementation of restoration and synchronization signals in the secondary control level.

3. RESULTS AND DISCUSSION

In this study, a typical microgrid with three distributed resources, two nonlinear loads, and one linear load is simulated in the MATLAB/Simulink to assess the efficiency of the proposed hierarchical-based control structure and evaluate their transition behavior in grid-connected and islanding mode operations. The test system under analysis and simulations is presented in Figure 8. Here, as energy resources, three 2.5 kVA VSIs are employed which are powered by three 650-DC voltage sources. The parameters of MG DG units and loads are represented in Table 1.

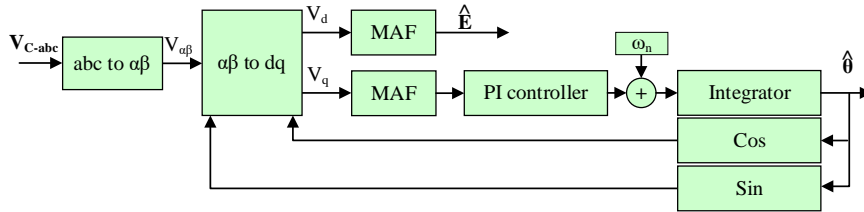


Figure 6. The SRF-PLL block diagram with in-loop MAF

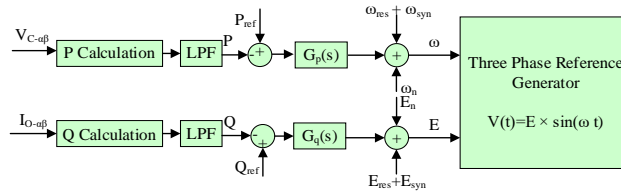


Figure 7. The restoration and synchronization block diagram in droop

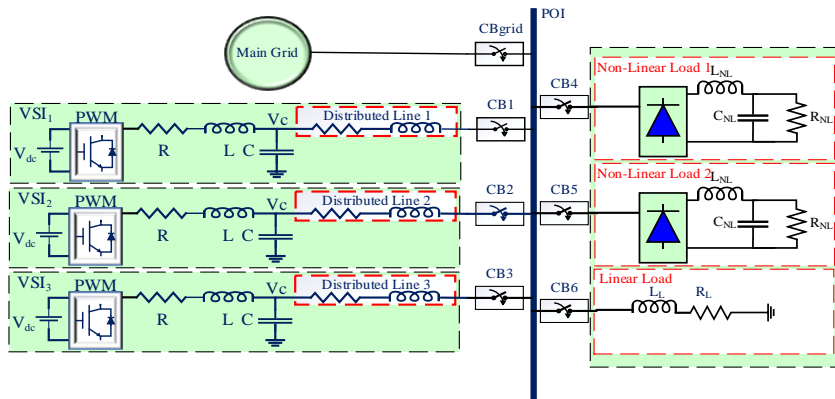


Figure 8. The test system under analysis and simulations

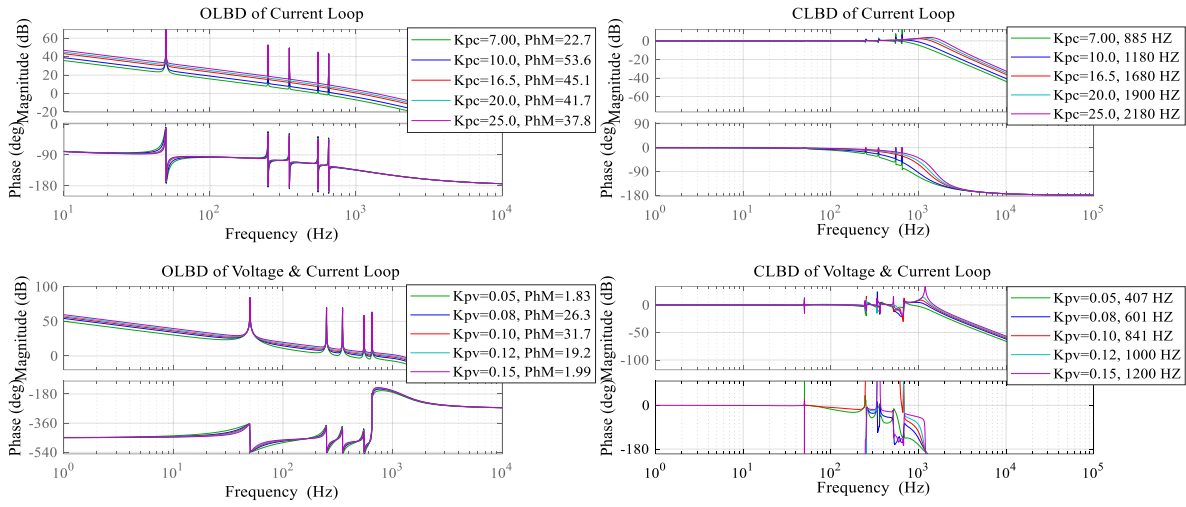


Figure 9. The bode plots of the internal and external loop of the inner level to design voltage and current controllers

TABLE 1. Load characteristics, power stage, and control parameters

LC Filters	$R = 0.02 \Omega$, $L = 1.8 \text{ mH}$, $C = 25 \mu\text{F}$
DC-Link Voltage	650V
Switching Frequency	10 kHz
DG Feeder	$R_F = 0.2 \Omega$, $L_F = 1.5 \text{ mH}$,
Main Grid (V/F)	400 V (line-line – RMS)/50 Hz
Linear Load	$R_L = 200 \Omega$, $L_L = 5 \text{ mH}$
Nonlinear Loads	$R_{NL} = 100 \Omega$, $L_{NL} = 0.84 \text{ mH}$, $C_{NL} = 235 \mu\text{F}$

Figure 9 is represented the bode plots of the internal loop and external loop to allocate voltage and current controller parameters. The behavior of variations of K_{pc} and K_{pv} on system phase stability margin in the internal and external loops are represented, there. By tuning the value of $K_{pc}=16.5$ and according to 10 kHz of the VSI switching frequency, the bandwidth and phase margin in the internal loop are achieved 1.68 kHz and 45.1° , respectively. These values can stable the current control system. As is mentioned before, to set the parameter of controllers and abstinence of interference, the internal loop should be faster than the external one. Then, by setting the value of K_{pv} in the external loop, 841 kHz for the bandwidth and 31.7° for the phase margin are achieved which can make a stable voltage control system. Besides, fundamental and harmonic orders (5th, 7th, 11th, and 13th) tracking will occur in both internal and external loops and approved that the controllers are well-analyzed to designed. Furthermore, Table 2 is presented the PR control parameters of internal and external loops. As the presence of nonlinear load leads to disturbed voltage, subsequently the input of standard SRF-PLL is a disordered signal.

TABLE 2. Proportional and multi-resonance current and voltage control parameters

K_{pc} , K_{rch5} , K_{rch5} , K_{rch7} , K_{rch11} , K_{rch13}	16.5, 200, 150, 150, 150, 150
K_{pv} , K_{rvh5} , K_{rvh5} , K_{rvh7} , K_{rvh11} , K_{rvh13}	0.10, 15.5, 15, 15, 15, 15

Therefore, on the base of Equations (19)-(21), the presence of (h)th order harmonic there causes (h – 1)th order disturbance component in the control loop of PLL.

$$E_a(t) = E_1 \cos \varphi_f + E_h \cos \varphi_h$$

$$E_b(t) = E_1 \cos(\varphi_f - 2\pi/3) + E_h \cos(\varphi_h - 2\pi/3) \quad (19)$$

$$E_c(t) = E_1 \cos(\varphi_f + 2\pi/3) + E_h \cos(\varphi_h + 2\pi/3)$$

$$E_d(t) = E_1 \cos(\varphi_f - \varphi) + E_h \cos(\varphi_h - \varphi) \approx E_1 - E_h \quad (20)$$

$$E_q(t) = E_1 \sin(\varphi_f - \varphi) + E_h \sin(\varphi_h - \varphi) \approx E_1(\varphi_f - \varphi) - E_h(\varphi_h - \varphi) \quad (21)$$

Therefore, harmonic orders of (–5, + 7, – 11, + 13, etc.), in the input of the SRF-PLL will appear as harmonic orders of (–6, + 6, – 12, + 12, etc.) in the PLL control loop. Likewise, the moving average filter which is a linear-phase low pass filter is applied in this study. Then, the DC component is passed and all harmonics whose frequencies are integer multiples of $1/T_w$ (T_w is the period of fundamental voltage) are entirely blocked. In the case of 50 Hz, harmonics up to the aliasing frequency are blocked (i.e. 50, 100, 150 Hz, etc). Furthermore, by considering $T_w=T/2$, all even-order harmonics up to the aliasing frequency (i.e. 100, 200, 300 Hz, etc) are blocked. Table 3 summarized the parameters of the SRF-PLL with in-loop MAF which is designed in our last study [8] and is modified and implemented, here.

TABLE 3. SRF-PLL within loop MAF parameters

T_w	0.02, S
$K_{p, PLL}$	82.8427
$K_{i, PLL}$	2.8427e+03, s^{-1}

TABLE 4. DGs Droop control parameters

K_{pp}, K_{ip}	1.142×10^{-4} (Ws/rd), 0.9×10^{-3} , (W/rd)
K_{pq}, K_{iq}	0.531×10^{-1} (VAR/V), 1.00 (VARs/V)

TABLE 5. Selective harmonic virtual impedance parameters

$R_{v,f}^+, L_{v,f}^+, R_{v,h} (-5, 7, -11, 13)^{th}$	0.5 Ω , 0.01 H, 1.0 Ω
---	-------------------------------------

TABLE 6. Synchronization and restoration PI and adaptive PI controller parameters

$K_{PF,syn}, K_{IF,syn}$	0.0001, 10 s^{-1}
$K_{PE,syn}, K_{IE,syn}$	0.0015, 0.00001 s^{-1}
$K_{PF,sec}, K_{IF,sec}$	1.25, 0.83 s^{-1}
$K_{PE,sec}, K_{IE,sec}$	1.0, 0.075 s^{-1}
$K_{PF,Adap-sec}, K_{IF,Adap-sec}$	1.8, 4.83 s^{-1}
$K_{PE,Adap-sec}, K_{IE,Adap-sec}$	3.5, 10.075 s^{-1}

As shown in Figure 8, the capacitor inside the nonlinear loads can make an inrush current. Then, the transition in the time of system variations such as load connection/disconnection depends on its capacitor initial charge. Therefore, to limiting them which causes the inrush current of the capacitor, two-step series resistors are used for a short time (0.3 s). Here, two cases are studied to prove the proficiency of this research in MATLAB/Simulink.

Case study 1: three DGs are considered as MG and are responsible for injecting the active and reactive power to the power system and support local linear and nonlinear loads (as sensitive loads). In this case. it should be mentioned that the contribution of all DG units is considered equal. Consequently, the hierarchical-based control structure of three-phase VSIs in a type of MG is implemented to make a seamless transition in system variations and make harmonic compensation by proportional and multi-resonant voltage and current controllers. Also, SRF-PLL with in-loop MAF is used to prepare the V/F extraction of the VSIs and enhance the simulation results.

Case study 2: In this case, to consider the robustness of the hierarchical control more, it is assumed that the impedance line of DG₃ is twice the others. Also, the effect of implementing the adaptive secondary control in MG restoration is considered. Besides, to have better and

decoupled harmonic power-sharing, selective harmonic virtual impedance is implemented.

As presented in Table 7, the simulation schedule is as follows: in T_1 , the DGs synchronization of the VSIs are started. After DGs synchronization, the DGs are connected, and an MG is created. Then, MG synchronization starts in T_2 until T_3 to synchronize them to the main grid. In T_3 , microgrid synchronization is finished and the microgrid is coupled to the upstream grid and is injected pre-planned power to them, simultaneously. Then, in T_4 and T_5 , the local sensitive loads are linked, respectively. Soon after, unintended islanding of the MG has happened and the microgrid is responsible to support the local loads in T_6 . Finally, in T_7 , an unintentional outage occurs for DG₃ while other DGs are in control to support sensitive loads.

The simulation results of the frequency and maximum voltage amplitude waveforms of the VSIs in case 1 are represented in Figure 10. Likewise, Figure 11 is represented the controlled power-sharing of the DGs. As is shown there, all the DGs were injecting pre-planned power to the upstream grid (1350 W-450 VAR) by themselves at T_3 and after that, they support local sensitive loads which are linear and nonlinear at T_4 and T_5 , respectively. Next, the MG is suddenly isolated at T_6 , and accordingly, the exchanged power between the MG and the upstream power system is becoming zero. So, the MG should support local and sensitive loads, lonely. Also, an unintentional outage of DG₃ happens at T_7 . In this case study, the parameters of all DGs and transmission lines are the same. In this paper, the advanced SRF-PLL with in-loop MAF which has higher disturbance rejection ability is employed, as well. It contains filters in the SRF-PLL to pass the DC component of the signals and filters the harmonic. Finally, as is showed in the achieved results of case 1, the seamless transitions from grid-connection mode to islanded mode, load variation, and distributed resource outage are attained. Plus, the harmonics compensation is implemented by the PR controller which is reported in Table 8. In case 2, to make more decoupled harmonic power-sharing in a system with nonlinear loads, a selective harmonic virtual impedance is implemented, too. Moreover, to cover the local grid variation in IM, a

TABLE 7. simulation schedule

Operation mode	Time (s)
time to start DGs synchronization	$T_1 = 0.0$
time to end of DGs synchronization and connection, time to start MG synchronization to the grid	$T_2 = 1.0$
time to end of MG synchronization, MG to grid connection, power injection to the main grid	$T_3 = 2.0$
time for connecting a linear local load	$T_4 = 3.5$
time for connecting nonlinear local loads 1, 2	$T_5 = 4.0$
time for unintentional islanding of MG	$T_6 = 5.0$
time for the unplanned outage of DG ₃	$T_7 = 6.5$

simple adaptive secondary control is applied instead of general secondary control implemented in case 1 which is based on a two-step lookup table. Figure 12 is represented the measured voltage and frequency of the DGs by SRF-PLL with in-loop MAF. As is mentioned before, in this section, to consider the capability of the hierarchical control during system variation, it is assumed that the impedance line of DG₃ is twice the others. The effect of them is on DGs power-sharing. Figure 13 is shown the comparison of voltage and frequency in both cases 1 and 2. Although the behavior of control is acceptable in case 1, the control is more

complicated in case 2. But the better seamless transition in voltage and frequency has happened which is shown in Figure 13.

Besides, Figure 14 is presented the decoupled active and reactive power shared by the DGs of the microgrid in case 2. As it is depicted there, in IM, although the droop coefficients of all DGs are the same, the reactive power is not shared equally between the DGs for the reason of the feeder line impedance mismatch and voltage drop in the feeder. Also, Figure 15 represents the injected current of the DGs to the PCC and main grid.

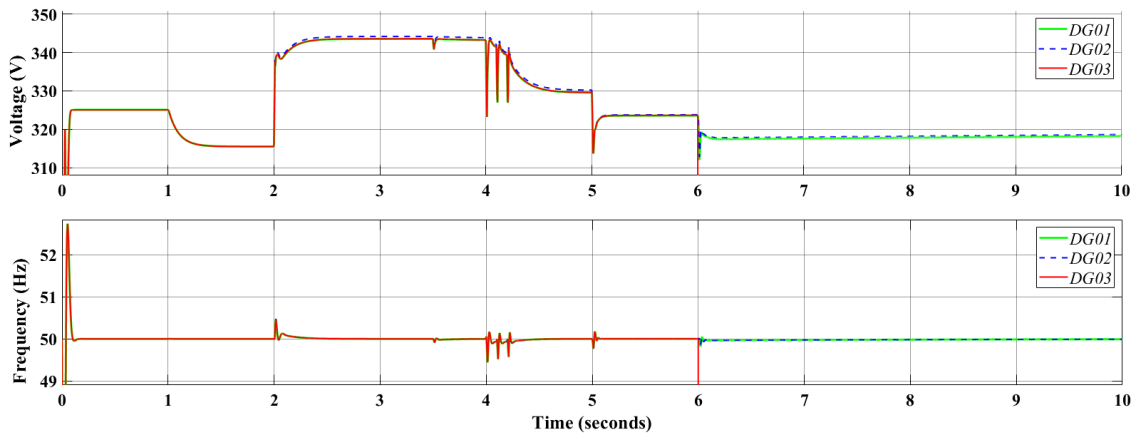


Figure 10. Simulation results of the frequency/voltage of the MG by SRF-PLL with in-loop MAF in Case 1

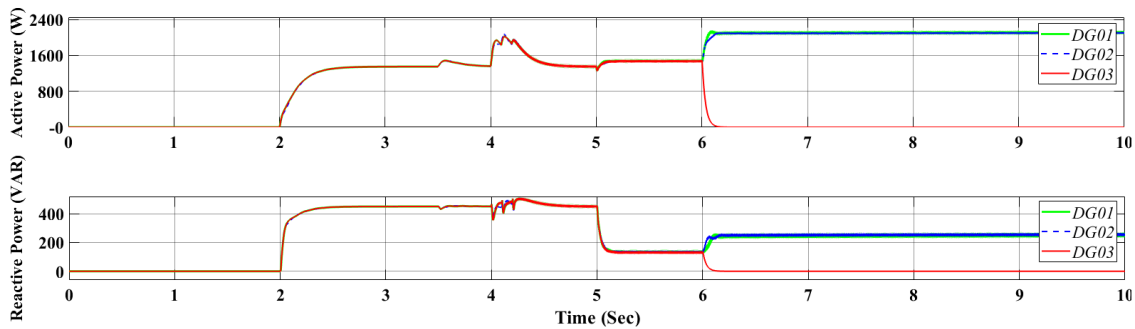


Figure 11. The controlled active and reactive power-sharing in the VSIs of the MG in case 1

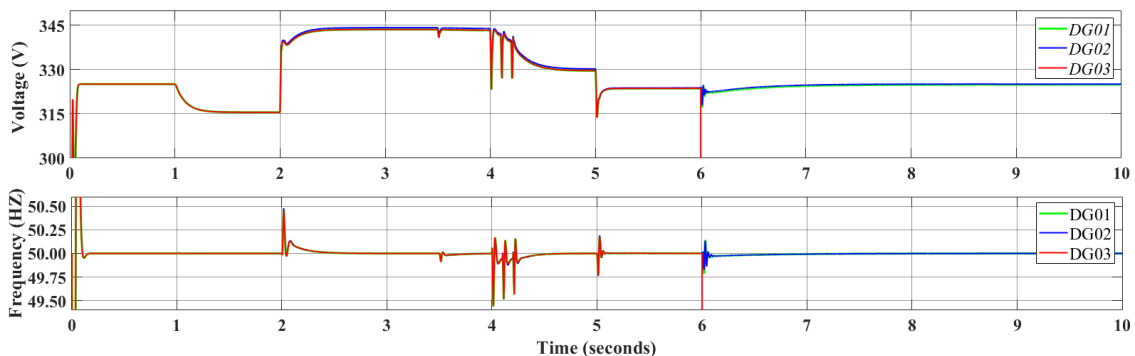


Figure 12. The simulation results of the frequency/voltage of the MG by SRF-PLL with in-loop MAF in Case 2

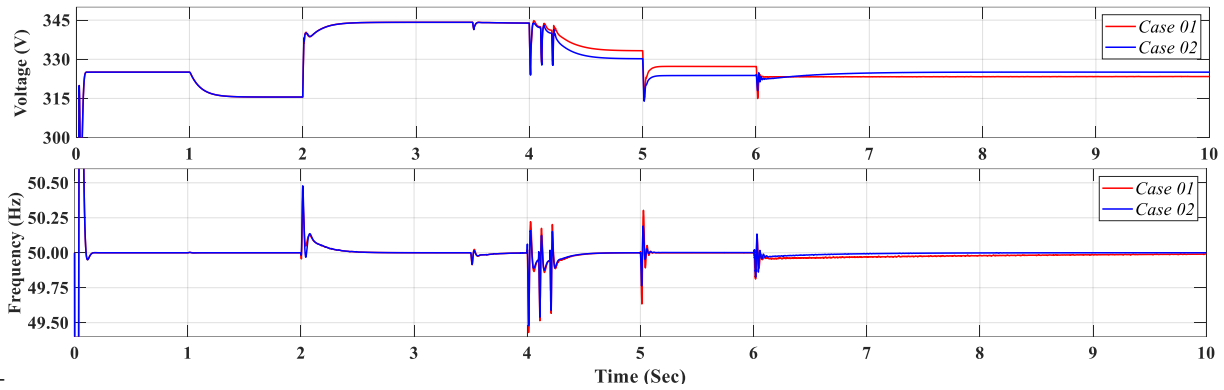


Figure 13. A comparison between different control approaches in voltage/frequency of the MG in Cases 1 and 2

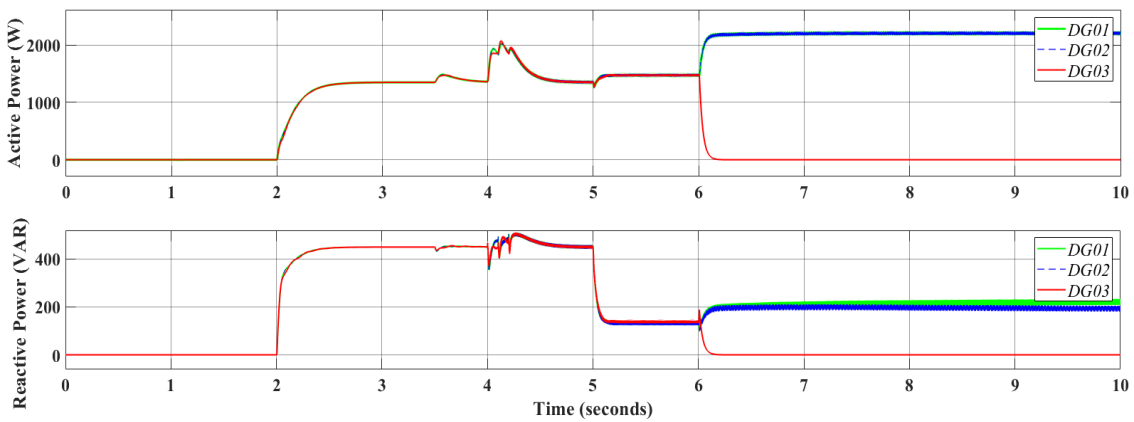


Figure 14. The controlled active and reactive power-sharing in the VSIs of the MG in case 2

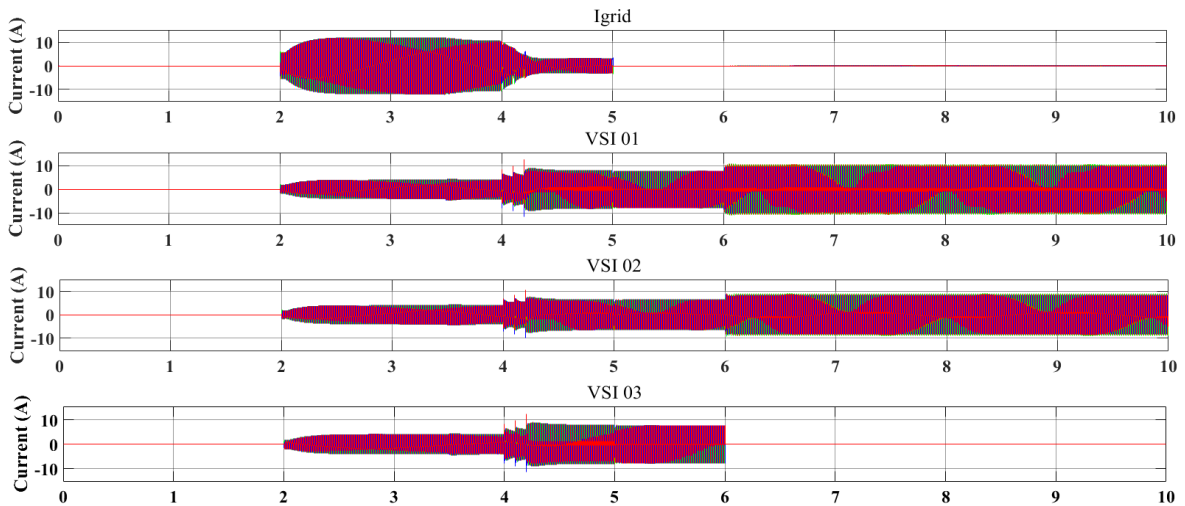


Figure 15. Three-phase injected current waveform to the PCC and main grid in case study 2

As the results are presented for both case studies in Figure 16, it is demonstrated that by applying SHVI in the primary control level of MG, hierarchical based control structure and adaptive secondary control, proper harmonic power-sharing and harmonic compensation along with seamless transition during grid variation are achieved.

4. CONCLUSION

This paper represented an enhanced control strategy based on hierarchy to enhance AC MG stability and make the seamless transition along with unintentional variation in the power systems. In the proposed structure, the PR controllers based on $\alpha\beta$ frame are implemented to ensure

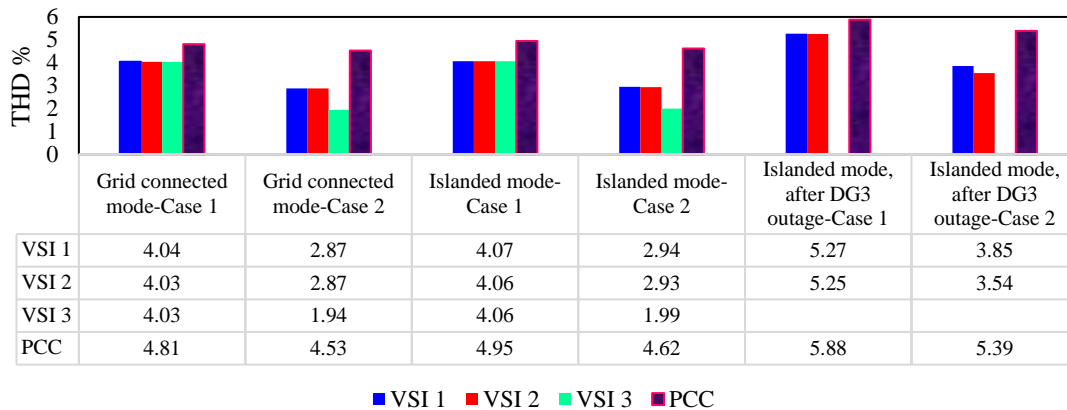


Figure 16. The THD (%) variation of the voltage in different operation modes

the stability and make compensation of harmonic while selective harmonic virtual impedance and MSOGI in the level of primary, simple adaptive lookup table restoration loop and advanced three-phase synchronous reference frame phase locked-loop with in-loop MAF in the level of secondary are incorporating to damp variation and transition more. Here, the control performance is investigated by using grid dynamics such as unplanned islanding, loads dynamic, nonlinear loads existence, and DG's outages which may cause the insecure MG operation. Furthermore, an AC MG with interface three-phase PWM VSI is considered to confirm the efficacy of the planned control scheme and the simulation results denoted that the strategy has high performance in compensation of THD, robustness in controllability, seamless transition during variation of system configuration. The future work of this study will be extended to propose a novel and user-friendly controller based on delay control instead of the PR controller to control of microgrid.

5. REFERENCES

- Palizban, O. and Kauhaniemi, K., "Hierarchical control structure in microgrids with distributed generation: Island and grid-connected mode," *Renewable and Sustainable Energy Reviews*, Vol. 44, 797-813, (2015), DOI: 10.1016/j.rser.2015.01.008.
- Li, X., Zhang, H., Shadmand, M.B., and Balog, R. S., "Model predictive control of a voltage-source inverter with seamless transition between islanded and grid-connected operations," *IEEE Transactions on Industrial Electronics*, Vol. 64, No. 10, 7906-7918, (2017), DOI: 10.1109/TIE.2017.2696459.
- Meng, L., Savaghebi, M., Andrade, F., Vasquez, J. C., Guerrero, J. M., and Graells, M., "Microgrid central controller development and hierarchical control implementation in the intelligent microgrid lab of Aalborg University," 2015 IEEE Applied Power Electronics Conference and Exposition (APEC), 2585-2592, (2015), DOI: 10.1109/APEC.2015.7104716.
- Kaur, A., Kaushal, J., and Basak, P., "A review on microgrid central controller," *Renewable and Sustainable Energy Reviews*, Vol. 55, 338-345, (2016), DOI: 10.1016/j.rser.2015.10.141.
- Guerrero, J. M., Chandorkar, M., Lee, T. and Loh, P. C., "Advanced Control Architectures for Intelligent Microgrids—Part I: Decentralized and Hierarchical Control," *IEEE Transactions on Industrial Electronics*, Vol. 60, No. 4, 1254-1262, (2013), DOI: 10.1109/TIE.2012.2194969.
- Farokhian Firuzi, M., Roosta, A., and Gitizadeh, M., "Stability analysis and decentralized control of inverter-based ac microgrid," *Protection and Control of Modern Power Systems*, Vol. 4, (2019), 10.1186/s41601-019-0120-x.
- Rocabert, J., Luna, A., Blaabjerg, F., and Rodriguez, P., "Control of power converters in AC microgrids," *IEEE Transactions on Power Electronics*, Vol. 27, No. 11, 4734-4749, (2012), DOI: 10.1109/TPEL.2012.2199334.
- Norozpour Niazi, A., Vasegh, N., and Motie Birjandi, A. A., "To study unplanned islanding transient response of microgrid by implementing MSOGI and SRF-PLL based hierarchical control in the presence of nonlinear loads," *IET Renewable Power Generation*, Vol. 14, No. 5, 881-890, (2020), 10.1049/iet-rpg.2019.0506.
- Guerrero, J. M., Vasquez, J. C., Matas, J., de Vicuna, L. G. and Castilla, M., "Hierarchical Control of Droop-Controlled AC and DC Microgrids: A General Approach Toward Standardization," *IEEE Transactions on Industrial Electronics*, Vol. 58, No. 1, 158-172, (2011), DOI: 10.1109/TIE.2010.2066534.
- Sedhom, B. E., El-Saadawi, M. M., Hatata, A. Y., and Abd-Raboh, E. H. E., "H-infinity versus model predictive control methods for seamless transition between islanded- and grid-connected modes of microgrids," *IET Renewable Power Generation*, Vol. 14, No. 5, 856-870, (2020), DOI: 10.1049/iet-rpg.2019.0018
- Moradi, M. H., Eskandari, M., and Siano, P., "Safe transition from connection mode to islanding mode in microgrids," 24th Iranian Conf. on Electrical Engineering (ICEE), 1902-1907, (2016), DOI: 10.1109/IranianCEE.2016.7585832.
- Li, Y., Yuan, L., Meng, K., and Dong, Z., "Smooth states transition control strategy for microgrid," IEEE Int. Conf. on Information and Automation (ICIA), 86-91, (2017), DOI: 10.1109/ICInfA.2017.8078887.
- Lavanya, V., and Senthil Kumar, N., "Seamless Transition in Grid-connected Microgrid System using Proportional Resonant Controller," *International Journal of Engineering*, Vol. 33, No. 10, 1951-1958, (2020), DOI: 10.5829/IJE.2020.33.10A.13.
- Ahmadi, M., Sharafi, P., Mousavi, M. H., and Veysi, F., "Power Quality Improvement in Microgrids using STATCOM under Unbalanced Voltage Conditions," *International Journal of Engineering, Transactions C: Aspects*, Vol. 34, No. 6, 1455-1467, (2021), DOI: 10.5829/IJE.2021.34.06C.09.
- Imran, R. M., Wang, S., Flaih, F. M. S., and Salih, H. W., "Smooth mode transition control for micro-grid with hybrid battery/diesel combination," 4th International Conference on Information Science

- and Control Engineering (ICISCE), 1237-1242, (2017), DOI: 10.1109/ICISCE.2017.257.
16. Golestan, S., Monfared, M., and Freijedo, F. D., "Design-oriented study of advanced synchronous reference frame phase-locked loops," *IEEE Transactions on Power Electronics*, Vol. 28, No. 2, 765-778, (2013), DOI: 10.1109/TPEL.2012.2204276.
 17. Golestan, S., Guerrero, J. M., and Vasquez, J. C., "A PLL-based controller for three-phase grid-connected power converters," *IEEE Transactions on Power Electronics*, Vol. 33, No. 2, 911-916, (2018), DOI: 10.1109/TPEL.2017.2719285.
 18. Golestan, S., Guerrero, J. M., Vidal, A., Yepes, A. G., and Doval-Gandoy, J., "PLL with MAF-based prefiltering stage: small-signal modeling and performance enhancement," *IEEE Transactions on Power Electronics*, Vol. 31, No. 6, 4013-4019, (2016), DOI: 10.1109/TPEL.2015.2508882.
 19. Golestan, S., Guerrero, J. M., Vasquez, J. C., Abusorrah, A. M., and Al-Turki, Y., "A study on three-phase FLLs," *IEEE Transactions on Power Electronics*, Vol. 34, No.1, 213-224, (2019), DOI: 10.1109/TPEL.2018.2826068.
 20. Vasquez, J. C., Guerrero, J. M., Savaghebi, M., Eloy-Garcia, J. and Teodorescu, R., "Modeling, Analysis, and Design of Stationary-Reference-Frame Droop-Controlled Parallel Three-Phase Voltage Source Inverters," *IEEE Transactions on Industrial Electronics*, Vol. 60, No. 4, 1271-1280, (2013), DOI: 10.1109/TIE.2012.2194951.
 21. He, J., Li, Y. W., and Blaabjerg, F., "Flexible Microgrid Power Quality Enhancement Using Adaptive Hybrid Voltage and Current Controller," *IEEE Transactions on Industrial Electronics*, Vol. 61, No. 6, 2784-2794, (2014), DOI: 10.1109/TIE.2013.2276774.
 22. Han, Y., Shen, P., Zhao, X., and Guerrero, J. M., "An enhanced power-sharing scheme for voltage unbalance and harmonics compensation in an islanded AC microgrid," *IEEE Transactions on Energy Conversion*, Vol. 31, No. 3, 1037-1050, (2016), DOI: 10.1109/TEC.2016.2552497.
 23. Savaghebi, M., Jalilian, A., Vasquez, J. C., and Guerrero, J. M., "Secondary control for voltage quality enhancement in microgrids," *IEEE Transactions on Smart Grid*, Vol. 3, No.4, 1893-1902, (2012), DOI: 10.1109/TSG.2012.2205281.
 24. Yazdani, A., Iravani, R., "Voltage-Sourced Converters in Power Systems: Modeling, Control, and Applications," *Wiley-IEEE Press*, 2010.
 25. Rocabert, J., Luna, A., Blaabjerg, F., and Rodríguez, P., "Control of Power Converters in AC Microgrids," *IEEE Transactions on Power Electronics*, Vol. 27, No. 11, 4734-4749, (2012), DOI: 10.1109/TPEL.2012.2199334.
 26. Zamora, R. and Srivastava, A. K., "Controls for microgrids with storage: review, challenges, and research needs," *Renewable and Sustainable Energy Reviews*, Vol. 14, No. 7, 2009-2018, (2018), DOI: 10.1016/j.rser.2010.03.019.
 27. Golsorkhi, M. S. and Savaghebi, M., "A Decentralized Control Strategy Based on V-I Droop for Enhancing Dynamics of Autonomous Hybrid AC/DC Microgrids," *IEEE Transactions on Power Electronics*, Vol. 36, No. 8, 9430-9440, (2021), DOI: 10.1109/TPEL.2021.3049813.
 28. Mousazadeh Mousavi, S. Y., Jalilian, A., Savaghebi, M., and Guerrero, J. M., "Coordinated control of multifunctional inverters for voltage support and harmonic compensation in a grid-connected microgrid," *Electric Power Systems Research*, Vol. 155, 254-264, (2018), DOI: 10.1016/j.epsr.2017.10.016.
 29. Golestan, S., Guerrero, J. M., Vasquez, J. C., Abusorrah, A. M., and Al-Turki, Y., "Modeling, Tuning, and Performance Comparison of Second-Order-Generalized-Integrator-Based FLLs," *IEEE Transactions on Power Electronics*, Vol. 33, No. 12, 10229-10239, (2018), DOI: 10.1109/TPEL.2018.2808246.
 30. Rodriguez, P., Luna, A., Candela, I., Mujal, R., Teodorescu, R., and Blaabjerg, F., "Multiresonant Frequency-Locked Loop for Grid Synchronization of Power Converters Under Distorted Grid Conditions," *IEEE Transactions on Industrial Electronics*, Vol. 58, No. 1, 127-138, (2011), DOI: 10.1109/TIE.2010.2042420.
 31. Heydari, R., Khayat, Y., Naderi, M., Anvari-Moghaddam, A., Dragicevic, T. and Blaabjerg, F., "A Decentralized Adaptive Control Method for Frequency Regulation and Power Sharing in Autonomous Microgrids," 2019 IEEE 28th International Symposium on Industrial Electronics (ISIE), 2427-2432, (2019), DOI: 10.1109/ISIE.2019.8781102.
 32. Li, M., Gui, Y., Guan, Y., Matas, J., Guerrero, J. M. and Vasquez, J. C., "Inverter Parallelization for an Islanded Microgrid Using the Hopf Oscillator Controller Approach with Self-synchronization Capabilities," *IEEE Transactions on Industrial Electronics*, (2020), DOI: 10.1109/TIE.2020.3031520.

Persian Abstract

چکیده

در این پژوهش، کنترل سلسله مراتبی بهبود یافته ریزشبهه مبتنی بر کنترل‌کننده‌های تناسبی-چندگانه رزونانسی به منظور جبران‌سازی اغتشاشات هارمونیک ناشی از بارهای غیرخطی پیشنهاد شده است. همچنین گذارهای محتمل ریزشبهه، بویژه از حالات متصل به شبکه بالادست به حالت جزیره‌ای همراه با گذارهای برخواسته از خروج‌های ناخواسته ریزمنابع موجود در یک ریزشبهه مورد مطالعه قرار گرفته است. در اینجا، ساختار کنترل سلسله مراتبی پیشنهاد شده از سه سطح کنترلی تشکیل شده که شامل سطوح کنترلی داخلی، اولیه و ثانویه بر مبنای قاب مرجع ساکن می‌باشند. کنترل‌کننده‌های ولتاژ و جریان اینورترهای مبدل ولتاژی سه فاز که در سطح داخلی قرار گرفته‌اند، از نوع کنترل‌کننده‌های تناسبی-چندگانه رزونانسی می‌باشند. بعلاوه در سطح کنترل اولیه، از یک کنترل‌کننده آفتی همراه با امپدانس مجازی هارمونیک گزینشی برای رسیدن به تسهیم مناسب توان بین ریزمنابع استفاده شده است. به منظور رسیدن به بازیابی بهتر و گذار هموارتر در جزیره‌ای شدن‌های برنامه‌ریزی نشده، خروج‌های ناخواسته ریزمنابع موجود در یک ریزشبهه و فرایند همگام‌سازی، از یک فاز حلقه قفل شده توسعه یافته در قاب مرجع ساکن همراه با حلقه فیلتر میانگذر متحرک و یک کنترل‌کننده تطبیقی بر مبنای جدول مرجع ساده در سطح کنترلی ثانویه بهره گرفته شده است. نتایج شبیه‌سازی در محیط متلب/سیمولینک نشان داده که روش پیشنهاد داده شده بازدهی سیستم کنترل، موثر بودن آن و مقاوم بودن آن را در حین تغییرات در ساختار شبکه بهبود داده است.
